High-Field fMRI

4

Elke R. Gizewski

4.1 Introduction

In recent years, functional magnetic resonance imaging (fMRI) has become a widely used approach for neuroscience. However, this method has the potential to be improved with regard to both spatial and temporal resolution. The blood-oxygenation level-dependent (BOLD) contrast represents signal changes in T2- or T2*-weighted images. These sequences are presumed to be well suited to high magnetic field strength, as fMRI sequences benefit from higher signal-to-noise ratio (SNR) and higher signal in BOLD contrast images (Vaughan et al. 2001). However, their sensitivity to susceptibility also causes problems, e.g. in-plane dephasing and signal dropouts near tissue-air boundaries.

To achieve greater insights into brain function, ultra-high-field fMRI has been applied in some studies to attain higher spatial resolutions (Duong et al. 2003; Pfeuffer et al. 2002a). These studies focused on high-resolution images which can be acquired rapidly and with good temporal and special resolution. Additionally, the signal increase advantage in high-field MRI has been studied (Pfeuffer et al. 2002b). Nearly all of these early studies, therefore, accepted restrictions in the field of view and the number of slices for 7-T imaging and avoided areas near tissue-air boundaries. For broader application including presurgical fMRI and for analysing cognitive functions, however, a more extended coverage of the brain is needed to reveal network activation involving multiple areas. This chapter will give insights into the pros and cons of high- and ultra-high-field fMRI and into ongoing developments to overcome the restrictions referred to and improve the benefits.

4.2 Benefits and Limitations of High- and Ultra-High-Field MRI

The introduction of ultra-high-field MRI systems has brought MRI technology closer to the physical limitations, and greater development effort is required to achieve appropriate sequences and images. 3-T MRI systems are high-field systems maintaining a relatively high-comfort level for the user similar to 1.5-T MRI systems (Alvarez-Linera 2008; Norris 2003). Theoretically, the SNR at high-field MRI should, according to the Boltzmann equation, show a linear increase with increasing magnetic field strength. But, the interactions of the magnetic field and other influencing factors, e.g. relaxation times, radio frequency (RF) pulses and coils performance during image acquisition, are very complex. One important factor is the change in RF pulses in higher magnetic field strengths. Changing the field strength

E. R. Gizewski (✉)
Department for Radiology, University Clinic for Neuroradiology, Medical University Innsbruck, Innsbruck, Austria
e-mail: elke.gizewski@i-med.ac.at

S. Ulmer, O. Jansen (eds.), *fMRI*, https://doi.org/10.1007/978-3-030-41874-8_4

from 1.5 to 3 T results in a fourfold increase in the required energy, resulting in an increase in specific absorption rate (SAR) (Ladd 2007). The increase in SAR leads to limitations in image acquisition, as the absorption of energy in the tissue cannot be allowed to exceed certain thresholds. Therefore, restrictions in the number of slices and achieving homogenous excitation of the nuclei increase with higher field strength.

Current 3-T scanners have been significantly improved since their introduction, especially with regard to coil developments and sequence techniques; therefore, today the advantages, such as faster acquisition time and/or higher resolution, are greater than the disadvantages, such as higher costs and in some cases instability in running the systems (Scheef et al. 2007). For higher field strength, e.g. 7 T, the developments have also improved in the recent time but are still in the process of improvement.

Another important point is the magnet design. Especially at 7-T whole-body systems, the magnet is very long compared to a typical 1.5-T magnet. The bore is 60 cm as for a long time at common 1.5 T but due to the length gives a narrow impression (Fig. 4.1). Therefore, anxiety is again a problem for imaging. However, newer studies could demonstrate that the acceptance of 7-T imaging procedures in subjects and patients was acceptable (Theysohn et al. 2008). A final important point is the contraindication of every metal implant at 7 T. Even non-ferromagnetic material can be influenced due to induced electrical currents. When located in the centre of imaging, such material, e.g. a surgical calotte fixation, would lead to disturbing artefacts.

Some recent studies addressed the possible side effects of ultra-high-field MRI as increasing spread of high-field and ultra-high-field scanners has encouraged new discussion of the safety aspects of MRI. Studies on possible cognitive effects of MRI examinations could not reveal any significant influence of high field strength and the application of HF impulses during and after normal scanning procedures (Schlamann et al. 2010a). However, one study showed that immediately after MRI exposure, the cortical silent period during transcranial magnetic stimulation was highly significantly prolonged in normal subjects (Schlamann et al. 2010b). Interestingly this was found for 1.5 and 7 T with no significant difference or dependency on the field strength.

4.3 Special Aspects of High-Field fMRI

BOLD contrast images are normally acquired using a gradient echo-planar technique (EPI). Optimal sequence design has to take into account echo times and sampling period; the variation in sensitivity between tissues with different baseline T2∗, the effects of physiological noise and non-exponential signal decay are relevant influencing factors (Gowland and Bowtell 2007). In high-field fMRI, the optimal TE is shorter than at 1.5 T. The shortening of T2∗ is proportional to the magnetic field (Okada et al. 2005). The TE used in optimized 3-T fMRI imaging is between 30 and 35 ms (Preibisch et al. 2008). The optimum TE for 7 T has been reported to be around 25 ms in focused fMRI in the occipital cortex (Yacoub et al. 2001).

As mentioned above, the SNR should increase with the magnetic field strength. Some studies have revealed a BOLD signal increase up to fivefold in 7-T fMRI compared to 1.5-T BOLD signals. Studies focusing on an increase in resolution and small field of view (Pfeuffer et al. 2002c) could reveal a higher signal increase at 7 T than studies with whole-brain coverage (Gizewski et al. 2007). This variability can be explained taking into account the above-mentioned factors influencing the SNR. Additionally, the impact of these factors increases with higher field strength, resulting in a greater variability of BOLD signal between different measurements and subjects at 7 T compared to 1.5 T. The relatively wide range of relative BOLD signal changes compared to 1.5 T and even 3 T may also be explained by the difficulty in achieving a uniform static magnetic field shim and a uniform RF excitation field at 7 T. The fMRI experiments at 7 T are therefore more dependent on field inhomogeneities, and these have to be taken into account during image analysis.

Fig. 4.1 7-T MR scanner with a bore of 60 cm and a length of 3.50 m. The MR is surrounded by 425 tonnes of steel. The *upper figure* shows a person before positioned feet first into the scanner. The *lower figure* shows a person head first in the scanner with the head in the isocentre, the feet covered with a sheet. The scanner used here is located at the Erwin L. Hahn Institut, Essen, Germany

The BOLD effect at higher field strength increases less in vessels larger than the voxel size and is thus more pronounced in vessels smaller than the voxel size. By using smaller voxels at higher field strength compared to 1.5 T, the BOLD signal can become more specific and reliable (Shimada et al. 2008; Zou et al. 2005). Therefore, the signal changes should be more closely linked to the cortical activity. With the increasing signal and enhanced stability of the BOLD signal at higher field strength, the repetition of events can be reduced. At ultra-high fields, even single events can give reliable BOLD signal as discussed in more detail below (Sect. 4.5).

Recent studies have addressed further aspects of SNR and BOLD signal improvement: Newton et al. (2012) evaluated the potential benefits of higher fields for detecting and analysing functional connectivity. The authors measured the influence of spatial resolution (from 1-mm up to 3-mm slice thickness) during a motor task at 7 T on estimates of functional connectivity through decreased partial volume averaging. They could show that resting-state correlations within the

sensorimotor system increase as voxel dimensions decreased from 3 × 3 × 2 to 1 × 1 × 2 mm. These results suggest that the true representation of sensorimotor network is more focal than could be resolved with larger voxels. The authors conclude that the described increase may be due to decreased partial volume averaging and that functional connectivity within the primary seed region might be heterogeneous on the scale of single voxels.

A main problem at high field strength is the achievement of good response functions even in areas suffering from in-plane dephasing and signal dropouts near tissue-air boundaries. A further central problem is the increasing chemical shift, proportional to the magnetic field strength. All these limitations lead to errors when reading the echo. Therefore, the optimization of scanning parameters and coil construction is of much greater importance than in routine 1.5-T scanners. Today, many improvements are achieved and lead to increased use of 7 T for fMRI studies as discussed below. The following paragraphs will give some examples of these developments in ultra-high-field BOLD and structural imaging.

The shimming, especially at 7 T, should be performed manually by the user. Although the standard shimming algorithm may be used, multiple repetitions should be performed with close verification of the result before starting the EPI sequence. At higher field strengths, a per slice shimming may be necessary to account for increased B0 distortions. Additionally, the phase correction parameters can be calculated slice by slice using three non-phase-encoded navigator echoes before the EPI readout (Heid 1997). Excellent B0 homogeneity has been demonstrated recently in the human brain at 7 Tesla with the dynamic multi-coil technique (DYNAMITE) for magnetic field shimming (Juchem et al. 2011). Recently, this groups also report the benefits of DYNAMITE shimming for multi-slice EPI and T2∗ mapping (Juchem et al. 2015). Furthermore, high-degree and high-order B0 shimming was on gradient-echo EPI at 7 T with improvement especially for cortical regions (Kim et al. 2017). But also specially designed coils have been developed to overcome those limitations, e.g. multichannel-phased array transmit coils with homogenous excitation across the visual cortex (Sengupta et al. 2016).

Nevertheless, there are increased susceptibility artefacts at 3 and 7 T compared to 1.5 T. Significant improvement can be reached by using more advanced head coils than circularly polarized (CP) coils. Multichannel coils allow application of parallel acquisition techniques (Mirrashed et al. 2004). Multiple channels provide further increases in SNR and, coupled with parallel imaging, reduce artefacts, e.g. due to susceptibility differences near tissue-air boundaries as is known from experience at 1.5 T. It has been demonstrated that the use of parallel imaging at 3 T results in an increase of BOLD signal depending on the employed parallel imaging method and its implementation (Preibisch et al. 2008). At 7 T, the coil equipment has to be newly developed, as the 7-T MRI systems require combined transmit and receive (t/r) coils. The first t/r coils were CP designs which did not enable parallel imaging techniques, but multichannel designs with up to 32 receiver channels are now available. Some groups also design their own coils in respect to higher resolution using more than 32 channels. As multichannel t/r coils for 7 T are now available more easily, nearly all experimental groups switched from CP to multichannel coils.

A further disadvantage at high field could be a restriction in the number of slices due to SAR restrictions and inhomogeneous resolution over the brain (Wiggins et al. 2005). Therefore, the coils and sequences have to be chosen depending on the paradigms to be applied. Again, parallel imaging can be useful for reducing the RF load on the tissue and enabling more slices. It was shown that at 3 T, a reduction factor of 2 in parallel imaging can be used with only little penalty with regard to sensitivity (Preibisch et al. 2008).

Some problems in image distortion can be solved using spin-echo instead of gradient-echo EPI sequences, but they are, so far, not routinely used. The blood contribution that dominates Hahn spin-echo (HSE)-based BOLD contrast at low magnetic fields and degrades specificity is highly attenuated at high fields because the apparent T2 of venous blood in an HSE

experiment decreases quadratically with increasing magnetic field. In contrast, the HSE BOLD contrast increases supralinearly with the magnetic field strength. Yacoub et al. report the results of detailed quantitative evaluations of HSE BOLD signal changes for functional imaging in the human visual cortex at 4 and 7 T (Yacoub et al. 2003). They used the increased SNR of higher field strengths and surface coils to avoid partial volume effects. Furthermore, they could show that high-resolution acquisitions lead to a CNR increase with voxel sizes <1 mm^3. It was concluded that the high-field HSE fMRI signals originated largely from the capillaries and that the magnitude of the signal changes associated with brain function reached sufficiently high levels at 7 T to make it a useful approach for mapping on the millimetre to submillimetre spatial scale.

Recently, balanced-steady-state free precession (b-SSFP) fMRI was developed utilizing the passband of the b-SSFP off-resonance response to measure MR signal changes elicited by changes in tissue oxygenation during increases in neuronal activity. This sequence allows distortion-free full-brain coverage with only two acquisitions and is a candidate for improved fMRI also at 7 T. Malekian et al. (2018) used a non-balanced SSFP at 7 T with the conclusion that this sequence with suitable modifications can be regarded as a robust SSFP-based method for high spatial specificity fMRI techniques. Furthermore, a 3D-GRASE with variable flip angles was tested at 7 T fMRI (Kemper et al. 2016). The authors could show that variable flip angle refocusing schemes increase usability of 3D-GRASE for high-resolution f MRI as it results in a reduction of blurring and increase in spatial coverage. A further approach to overcome the distortion problem was the use of a T2-preparation module to induce BOLD contrast, followed by a single-shot 3D fast gradient-echo readout with short TE (Hua et al. 2014).

The problem that thermal and physiological noise dominates the SNR of the fMRI time course at high spatial resolutions at high field strengths can be a prominent issue if a high-resolution matrix and a thin slice thickness are used. The problem is acquiring data at lower resolution, which is then dominated by physiological noise. A solution would be to acquire data at high resolution and smooth the data back to the desired lower resolution. In such cases, the physiological noise can limit some benefits of high-field acquisition, since increases in image SNR produce only small increases in time course SNR if the 1.5-T resolution is used (Triantafyllou et al. 2006). But, some problems even at 3 T remain; low-frequency periodic fluctuations were found to have increased as well as the time-dependent increase in noise, especially in long EPI sessions (Shimada et al. 2008).

The Nyquist ghost also increases at higher field strength and is an important factor in BOLD imaging at 7 T. There are strategies to improve the traditional Nyquist ghost correction approach in EPI at high fields. One group describes schemes based on the reversal of the EPI readout gradient polarity for every other volume throughout an fMRI acquisition train as one improvement. The authors concluded that at high B0 fields, substantial gains in Nyquist ghost correction of echo-planar time series are possible by this alternating method (van der Zwaag et al. 2009).

The gradient-echo EPI sequences are mostly used for fMRI, especially for clinical applications. Therefore, the optimization of EPI sequences and reduction in artefacts are of great importance. Multichannel coils are basically an array of surface coils with higher signal in the periphery than in the centre. At higher field strength, the signal even in the centre of multichannel coils is higher compared to 1.5 T. Results obtained at 3 T using a combination of multichannel coil and parallel imaging showed that BOLD sensitivity improved by 11% in all brain regions, with larger gains in areas typically affected by strong susceptibility artefacts. The use of parallel imaging markedly reduces image distortion, and hence, the method has found widespread application in functional brain imaging (Poser et al. 2006). Recently, a new technique for 2D gradient-recalled gradient-echo EPI termed “variable slice thickness” (VAST) was introduced, which reduces signal losses caused

by through-slice susceptibility artefacts, while keeping the volume TR manageable (Brunheim et al. 2017).

A further interesting approach for BOLD imaging might be the three-dimensional segmented echo-planar imaging (3D-EPI). Single-shot EPI at 7 T often suffers from significant geometric distortions partly due to low bandwidth in the phase-encoded direction and amplified physiological noise. The 3D sequence could further improve high-resolution fMRI as it provides an increased SNR at similar temporal resolution to traditional multi-slice 2D-EPI readouts, in total, leading to increased volume coverage and decreased geometric distortions. The study of van der Zwaag et al. (2012) could reveal that during fMRI experiments at 7 T with a motor task, the 3D-EPI outperforms the 2D-EPI in terms of temporal SNR and sensitivity to detect activated brain regions. Similar results were reported in a further study using a 3D PRESTO sequence (Barry and Strother 2011).

In summary, an extended optimization of sequences and new coil developments, especially new transmit-receive coils, was done in the recent years with increasing evidence of optimized fMRI at ultra-high-field MRI. Furthermore, new aspects of multimodal imaging in functional MRI are more and more coming up. One example is the combination of neurochemical and BOLD MRI at 7 T. There are some reports about small concentration changes in lactate, glutamate, aspartate and glucose in the human cortex during prolonged stimuli. However, a correlation to BOLD-fMRI signals was unclear. Bednarik et al. (2015) could show that MRS at 7 T is sensitive to analyse such small signal changes and that BOLD-fMRI signals were positively correlated with glutamate and lactate concentration changes. As at 3 T and also at ultra-high-field MRI, the combination of DTI and fMRI is more and more used. For example, the functional specificity of the cortico-subcortical loops depending on varying levels of cognitive hierarchy as well as their structural connectivity was addressed using high-resolution fMRI and DTI (Jeon et al. 2014).

4.3.1 7 T and Beyond

The main driving force for the trend to higher and higher field strengths is the gain in intrinsic SNR, which is expected to grow at least linearly with field strength. However, as mentioned above, with increasing static field restrictions have to overcome, the homogeneity of the RF fields declines; the longitudinal relaxation time T1 increases, while T2 and T2∗ decrease; construction of RF coils for high frequencies becomes more and more important. An excellent overview of the development and comparison of 3 T, 7 T and 9.4 T is given by the paper of Pohmann et al. (2016). Their experiments could show that in standard experimental conditions, SNR increased supralinearly with field strength. But also, to take full advantage of this gain, the deteriorating B1 homogeneity and the decreasing T2 (∗) have to be overcome. Therefore, recent papers have described solutions for these challenges, for example, the higher-degree whole-brain B0 shimming at 9.4 T (Chang et al. 2018). They emphasized the necessity of calibrating the shim system and concluded that better B_0 homogeneity drastically reduces signal dropout and distortions for echo-planar imaging and significantly improves the linewidths of MR spectroscopy imaging. Similar to 7 T (as described above), a possible solution for fMRI is the use of SSFP imaging. First results have been presented for high-resolution mapping of neural activation in the visual brain areas at 9.4 T (Scheffler and Ehses 2016).

However, due to the mentioned increasing challenges at higher field strength, further studies and developments have to be done since we fully can take advantage of the high SNR increase at higher fields.

4.4 Ultra-High-Field fMRI: Recent Neurocognitive Studies

Early experiments have, besides motor paradigms, addressed retinotopic maps at 7 T. An identification of visual areas in the occipitoparietal cortex was found (Hoffmann et al. 2009). It was

demonstrated that the mean coherence increased with magnetic field strength and with voxel size. At 7 T, the occipital cortex could be sampled with high sensitivity in a single short session at high resolution. Therefore, retinotopic mapping at 7 T opens the possibility of detailed understanding of the cortical visual field representations and of their plasticity in visual system pathologies. A further study analysed the use of spin-echo BOLD with 1.8-mm resolution at 3- and 7-T imaging for retinotopic mapping in comparison to gradient sequences (Olman et al. 2010). As mentioned above, some early studies could demonstrate the use of spin-echo sequences for fMRI. Olman et al. could now show that GE BOLD and at 7-T SE BOLD had no systematic differences in either the area or the boundary locations for V1, V2 and V3. Therefore, the feasibility of high-resolution spin-echo BOLD experiments with good sensitivity throughout multiple visual areas was demonstrated. However, the highest resolution at ultra-high-field fMRI is restricted due to biological point-spread of the haemodynamic signal. The extent of this spread is described to be determined by the local vascular distribution and by the spatial specificity of blood flow regulation. Apart from this, there is influence from the measurement parameters. A recent study introduced a laminar surface-based analysis method and studied the relationship between spatial localization and activation strength as a function of laminar depth by acquiring an isotropic, single-shot EPI at 7 T (Polimeni et al. 2010). The BOLD signal was sampled exclusively from the superficial, middle or deep cortical laminae. This group could show that avoiding surface laminae improved spatial localization. They conclude that optimal spatial resolution in functional imaging of the cortex can be achieved using anatomically informed spatial sampling to avoid large pial vessels.

Apart from analyses of direct motor tasks as described in the clinical application discussion below, the sensorimotor network has recently been the focus on 7-T fMRI studies. Hale et al. used resting-state fMRI at 3 and 7 T to assess connectivity in the sensorimotor network and default mode network at different spatial smoothing levels (Hale and Brookes 2010). The authors found higher temporal correlation coefficients for both sensorimotor network and default mode network at 7 T compared to 3 T for all smoothing levels. The maximum physiological noise contribution was higher at 7 T. However, no significant difference in the spatial correlation of maps following physiological correction was found. Whole-brain high-resolution (down to 1-mm isotropic voxels) resting-state fMRI at 7 T using parallel imaging technology could be performed without restrictions in temporal resolution or brain coverage (De Martino and Esposito 2011). Since those first reports, further resting-state fMRI experiments have been published. For example, the higher resolution was used to characterize resting-state fMRI signal time course properties and evaluate different seed placements within and around haemorrhagic traumatic axonal injury lesions (Lee et al. 2018).

Up to now, some studies have and further studies will have to also address cognitive functions involving more challenging brain areas. One study evaluated BOLD responses due to visual sexual stimuli at 7 T (Walter et al. 2008). This study could demonstrate that fMRI at high fields provides an ideal tool to investigate functional anatomy of subcortical structures. Furthermore, due to an increased SNR, functional scans of short duration can be acquired at high resolution. Coming back to experiments involving areas with high sensitivity to susceptibility artefacts, first results revealed acceptable image quality using an 8-channel head coil at 7 T compared to 3 T (Fig. 4.2). Additionally, in these results, the hippocampal activation during a memory-encoding task improved from 3 to 7 T (Theysohn et al. 2013). However, the dropout of volunteers due to image inhomogeneities was higher at 7 T.

Using the above-mentioned improvements in BOLD imaging at 7 T, further studies were published addressing subregional network architecture. The medial temporal lobe substructures with its integral role in memory functions have been analysed using 7 T resting-state fMRI (Shah et al. 2018). They found a moderate structural and strong functional inter-hemispheric symmetry. Furthermore, several bilateral hippocampal

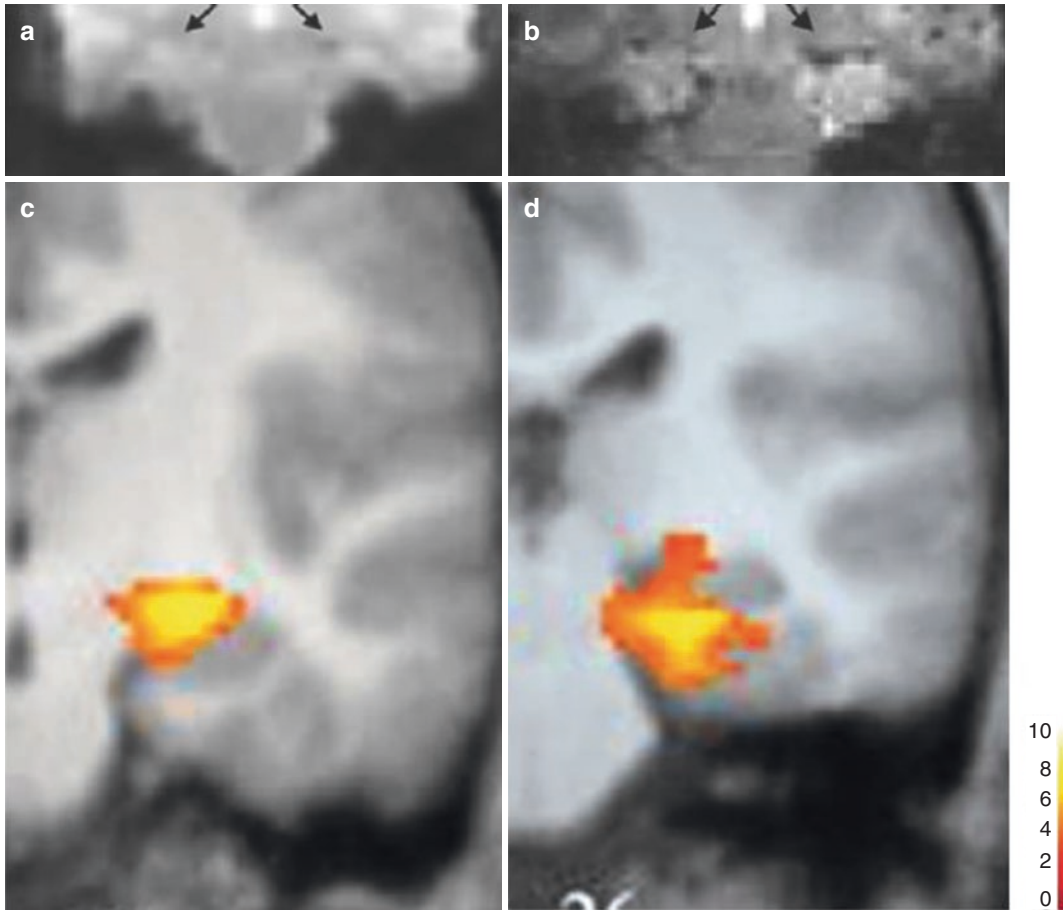

Fig. 4.2 EPI images with its sensitivity for susceptibility artefacts are compared at 3 T (**a**) and 7 T (**b**) imaging. Parallel acquisition techniques for reduction of these artefacts were used at both scanners (matrix 92 × 92 m^2 in this case at both scanners with 8-channel head coil). (**c** and **d**) The images show that the improvement of 7-T imaging techniques leads to acceptable image quality, allowing fMRI studies of the hippocampal region

subregions (CA1, dentate gyrus and subiculum) could be identified as functional network hubs. Another mapping was done using intraneural microstimulation of single mechanoreceptive afferent units in the median nerve in humans (Sanchez Panchuelo et al. 2016). With this method an opportunity is given to bridge the gap between first-order mechanoreceptive afferent input codes and their spatial, dynamic and perceptual representations in the human cortex. Another structure with small size and connection to other small regions, the bed nucleus of the stria terminalis was another target to use fMRI at 7 T (Torrisi et al. 2015). This region is implicated in the pathophysiology of anxiety and addiction disorders but easily addressed by conventional methods. This group used seed-based resting-state functional connectivity to map the bed nucleus resting-state network. They could demonstrate the in vivo reproduction of many human bed nucleus connections previously described in animal research.

4.5 Ultra-High-Field fMRI and Possible Clinical Applications

3-T fMRI is increasingly used in clinical and experimental studies in most countries. In addition to developments in coil technology, 3-T MRI provides an excellent solution for higher resolu-

tion and/or signal changes with an acceptable increase in susceptibility artefacts (Alvarez-Linera 2008).

3-T fMRI has been used in a variety of experiments so far. The initial dip in the motor and visual areas was examined simultaneously using a visually guided finger-tapping paradigm (Yacoub and Hu 2001). Other experiments could show that fMRI measurements quantifying the strength of activity and centres of mass in response to tasks offer sensitive measurements of change over repeated imaging sessions. Therefore, fMRI at high field strength can be used for serial investigations of individual participants using simple motor and cognitive tasks in a simple block design (Goodyear and Douglas 2008). These results are very promising in respect to advanced clinical use of high-field fMRI. At 1.5 T, one main problem is the restriction in obtaining individual activation maps due to lack of sensitivity and specificity. This can be overcome with the more stable haemodynamic response function and higher BOLD signal at 3 T and even more at higher field strength, e.g. 7 T.

Within the recent years, the number of fMRI studies using 3-T scanners has much grown as those scanners become more and more available. Besides experimental studies like evaluation of gender differences, encoding and recognition of pseudowords (Banks et al. 2012) or differences in humour (Kohn et al. 2011), clinical studies also revealed improvement of activation at 3 T compared to 1.5 T (Blatow et al. 2011). Figure 4.3 gives a typical clinical example of the use of 3-T (f)MRI in tumour patients. In the everyday setting, such significant activation during a finger-tapping task can be achieved robustly in a short block design and a scanner-associated post-processing with overlay on structural 3D T1 image after contrast application (MPRAGE). Recently, the mapping of substructures was published not only for visual and auditory cortex but also for human finger somatotopy ((Martuzzi et al. 2014). Cortical representations of fingers are of particular interest, and therefore these results have impact to clinical imaging.

The first 7-T studies were performed to demonstrate the feasibility of BOLD fMRI using EPI and to characterize the BOLD response in humans at 7 T using visual stimulation. These results indicate that fMRI can be reliably performed at 7 T and that at this field strength, both the sensitivity and spatial specificity of the BOLD response are increased. These studies suggest that ultra-high-field MR systems are advantageous for functional mapping in humans (Yacoub et al. 2001).

Decreasing the voxel size at high field strength and simultaneously obtaining high temporal resolution are major challenges and are mainly limited by gradient performance. Pfeuffer et al. used an optimized surface coil set-up for zoomed functional imaging in the visual cortex (Pfeuffer et al. 2002c). With a single-shot acquisition at submillimetre resolution ($500 \times 500\ mm^2$) in the human brain and a high temporal resolution of 125 ms, activation of single-trial BOLD responses was obtained. Therefore, the possibilities of event-related functional imaging in the human brain were expanded. One recent study in relation to brain-computer-interface (BCI) technology research used a real-time fMRI at 7 T to evaluate the potential benefit of this method for BCI interactions (Andersson et al. 2010).

For clinical use, the activation in eloquent areas such as the sensorimotor areas and coverage of larger brain volumes are of great importance. One study at 7 T revealed activation in all sensorimotor motor areas at 7 T: SI, MI, SII, SMA, thalamus and contralateral cerebellar areas involved in sensorimotor processing (Gizewski et al. 2007). Even when using a t/r CP coil, the signal change was a factor of 2–5 higher at 7 T than at 1.5 T. At 7 T, susceptibility artefacts were present especially in the basal brain structures, but a well-fitted response curve could be detected in all sensorimotor areas at 7 T, even in areas suffering from susceptibility such as the cerebellum (Fig. 4.4). In contrast to the results at 1.5 T, thalamic activation was found in all subjects and revealed an excellent response function. Even single-block analyses at 7 T revealed similar or even higher response strength than multi-block measurements at 1.5 T. These results indicate that fMRI can be robustly performed at 7 T, covering the whole brain using a t/r CP head coil with

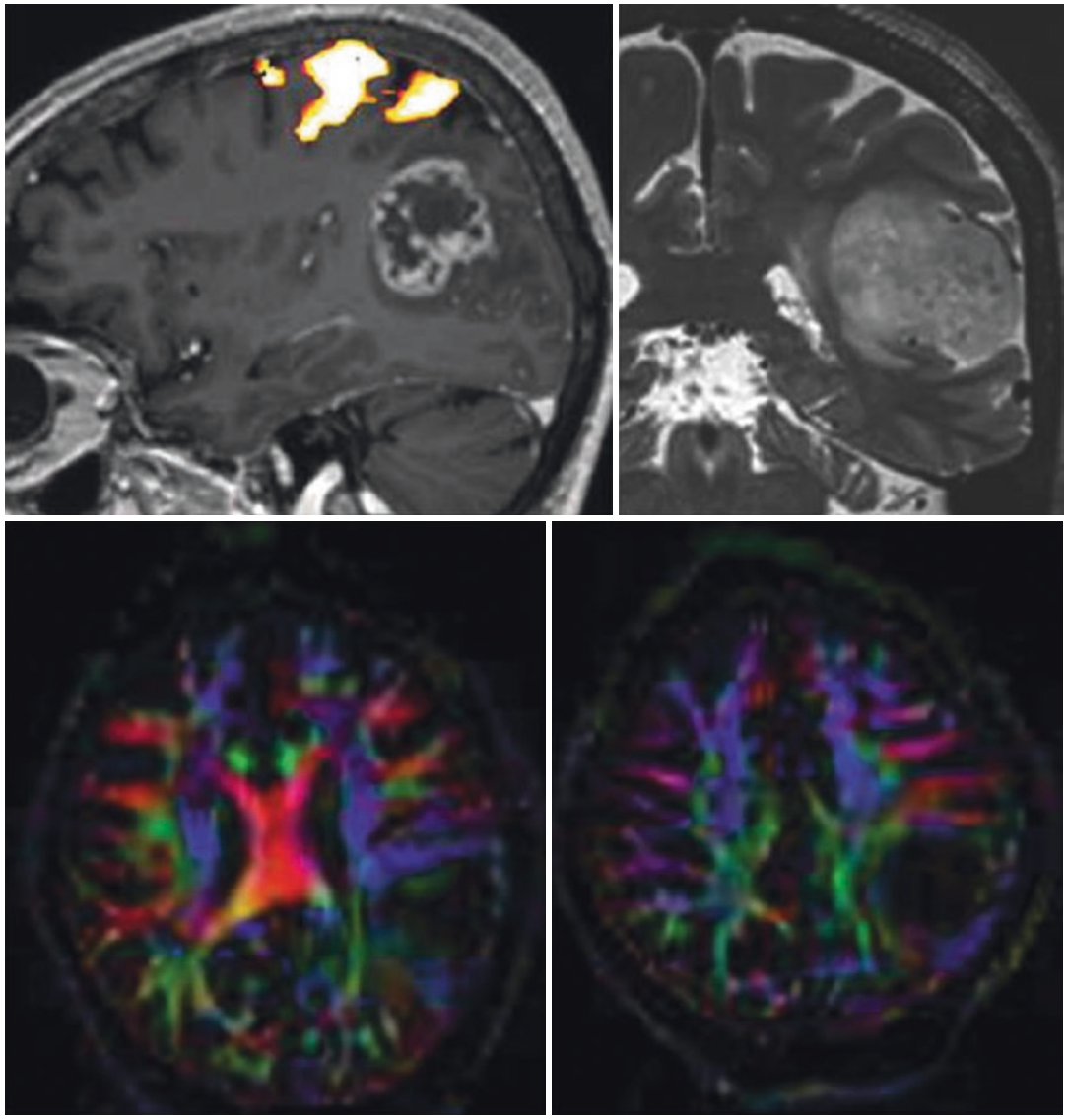

Fig. 4.3 Clinical application of 3 T: significant activation during a finger-tapping task performed by a patient with a brain tumour near the central area in a short block design. Results are presented after scanner-associated post-processing with overlay on structural 3D T1 image after contrast application (MPRAGE). In the same session, normally T2-weighted 3D images and a DTI are added to the fMRI task

higher signal and increased stability of the haemodynamic response curve. The excellent response functions and signal change elevations shown in this study using a well-established, simple sensorimotor paradigm indicate that even in susceptibility problematic brain regions, ultra-high-field fMRI is possible. A further study used a 16-channel head coil at 7 T to measure the topographic representation of the digits in human somatosensory cortex at 1-mm isotropic resolution in individual subjects (Sanchez-Panchuelo and Schluppeck 2010). This study using a tactile stimulation of each finger could show an orderly map of the digits on the postcentral gyrus. Those activations were robust and could be made in individual subjects, leading to a wide use of this method in clinical and experimental settings. These results are very interesting

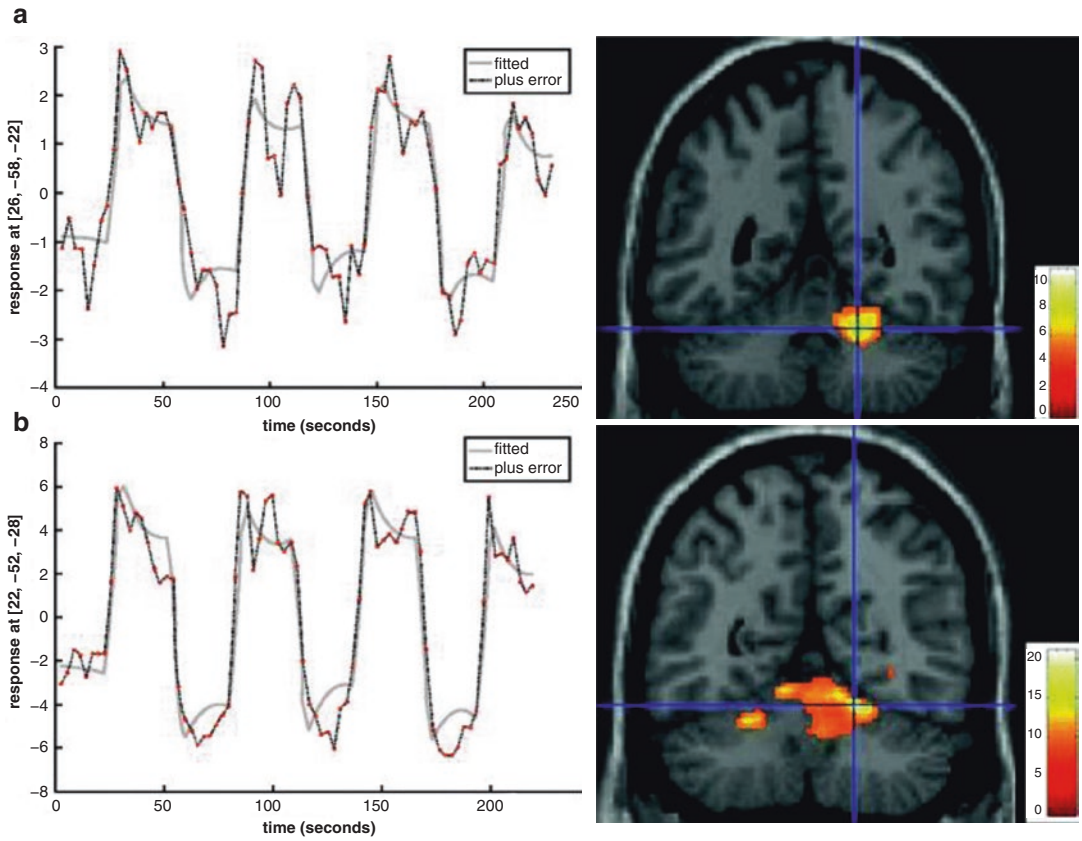

Fig. 4.4 (**a**) Plot of fitted response function at the main cluster in the cerebellar sensorimotor areas at 1.5 T (representative subject). Statistical parametric maps of activation within all subjects performing the finger-tapping task compared with rest period at 1.5 T. Task-related increase in MR signal is superimposed on coronal section of a 3D T1-weighted standard brain. Statistically corrected threshold is $p < 0.05$. Results show main activation in the cerebellum. (**b**) Plot of fitted response function at the main cluster in the cerebellar sensorimotor areas at 7 T (representative subject). Statistical parametric maps of activation within all subjects performing the finger-tapping task compared with rest period at 7 T. Statistically corrected threshold is $p < 0.005$. Results show main activation in the cerebellum

in relation to a similar study performed at 3 T (Olman et al. 2012). This group found strong evidence of BOLD selectivity in the hemisphere contralateral to the cued digit; however, they found no evidence for an orderly spatial topography. One can discuss the differences in respect to slight differing settings but also in respect to the influence of higher field strength.

As mentioned above the signal increase in ultra-high-field fMRI depends on many factors, not only on the magnetic field strength. Some studies have revealed a signal increase of up to fivefold using imaging parameters focused on increased spatial resolution and small field of view (Pfeuffer et al. 2002a, b). The sensitivity is somewhat constrained by the SNR characteristics if a CP head coil is used in conjunction with standard voxel sizes from 1.5 T. It has been shown that a reduction in voxel size leads to an improvement in time series SNR through a decrease in physiological noise (Triantafyllou et al. 2005). The relatively small BOLD changes in certain brain areas in the CP study might be explained by this effect, but the use of larger voxels allows whole-brain coverage.

It is likely that future studies will not strive for exceptional resolution in one area of the brain but be targeted at analysing complex networks.

Especially cognitive functions but also clinical applications require more slices and coverage of extended brain areas. Furthermore, some interesting structures such as the hippocampal region can, as in the cerebellum, suffer from signal dropouts near tissue-air boundaries. The recent developments in coil technique and sequences as well as post-processing have much improved the use of ultra-high field even in the mentioned problematic areas. Some examples were described in the cognitive section above. Figure 4.5 shows a further example with possible use not only in experimental settings but also in clinical applications: a representative activation of the dentate nucleus during a finger-tapping task. With such technique, even examination of activation of the dentate nucleus in a verb-generation task in normal volunteers was possible using the increase in signal-to-noise ratio (Thürling et al. 2011). For image processing, a newly developed region of interest-driven normalization method of the dentate nuclei was applied. This experiment suggests that the human dentate nucleus can be subdivided into a rostral and more dorsal motor domain and a ventrocaudal non-motor domain. Such findings represent the benefit of high-field fMRI with its higher SNR and possibility to reveal deep brain structures more reliable.

Further interesting structures with the need of higher resolution also in clinical applications are the brainstem and deep brain nuclei. This region also suffers from signal dropouts near tissue-air boundaries and pulsation artefacts, for example, due to the basilar artery (Fig. 4.6). For anatomical and fibre tracking methods (DTI), the sequences have been optimized resulting in depiction of substructures within the brainstem (Deistung et al. 2013, Gizewski et al. 2014). The anatomy of the human brainstem in vivo was mainly achieved by acquiring and generating images with multiple contrasts: T2/PD-weighted images,

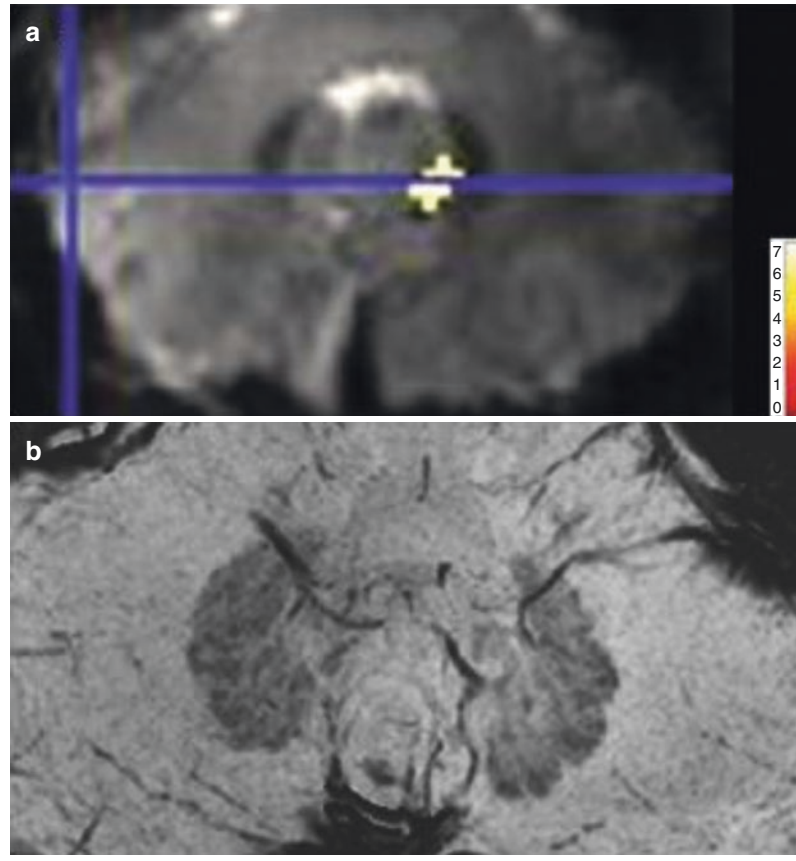

Fig. 4.5 Statistical parametric maps of activation of a single subject performing finger-tapping task compared with rest period at 7 T superimposed on EPI transverse orientation (**a**) and the high-resolution SWI imaging of dentate nucleus at 7 T (**b**). Statistically corrected threshold is $p < 0.001$

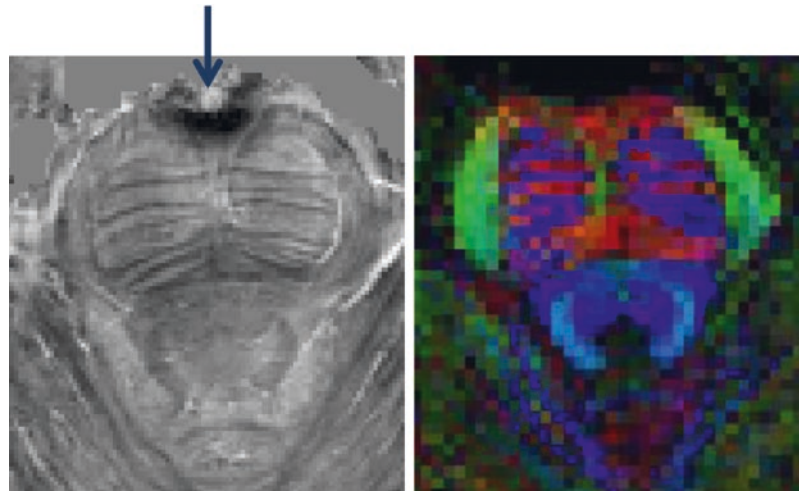

Fig. 4.6 SWI with pulsation artefact due to basilar artery, however, excellent resolution in DTI. Measurements in cooperation with Dr. Sina Straub, DKFZ, Heidelberg, Germany

quantitative maps of longitudinal relaxation rate (R1∗ maps), magnetic susceptibility maps (SWI with quantitative mapping) and DTI. For fMRI further challenges have to be solved in this region. The haemodynamic response function (HRF) may vary substantially in subcortical structures, and adoption in designing and interpretation of fMRI studies of these regions are needed. Lewis et al. (2018) studied the temporal properties and non-linearities of the HRF across the human subcortical visual system (superior colliculus, lateral geniculate nucleus of the thalamus, primary visual cortex). They concluded that subcortical visual structures exhibit fast and non-linear haemodynamic responses and that these dynamics enable detection of fast BOLD signals even within small deep brain structures when imaging at 7 T. The high-resolution structural images of the brainstem with delineation of brainstem nuclei were further used to identify seed regions in resting-state fMRI (Bianciardi et al. 2016). Here, the connectomes of 11 brainstem nuclei of the ascending arousal, motor and autonomic systems from 12 controls could be presented.

A further substructure of the brainstem, which can be clearly visualized at 7 T, is the periaqueductal grey, a key region in autonomic function. Some 3 T studies have shown involvement of this region in some autonomic functions, e.g. pain processing. However, to identify these subregions was still impossible. Faull et al. (2015) then showed deactivation in the lateral and dorsomedial columns of the PAG corresponding with short breath holds and cortical activations demonstrating the involvement of these subregions of PAG in the network of conscious respiratory control for the first time in humans.

Basal ganglia circuits are important in neurological disorders such as Parkinson's disease (PD) and target in advanced therapies such as deep brain stimulation (DBS). Knowledge about the connectivity of the human basal ganglia and thalamus has evolved over recent years but still suffers from restricted resolution and sensitivity in in vivo imaging. One group presented an imaging and computational protocol to overcome this problems (Lenglet et al. 2012). High-resolution structural and functional images were acquired with 7 T and revealed detailed structural and connectivity representations of the human basal ganglia and thalamus. These data provides more information on basal ganglia circuitry and has impact for pre-surgical planning in individual human subjects. This optimized fMRI for basal ganglia using a reduction of echo time and spatial resolution was used by de Hollander et al. (2017). They also revealed that an fMRI protocol at 3 T with identical resolution to the 7 T showed no robust BOLD sensitivity in any of the BG nuclei. Therefore, this application is a well-confirmed benefit of ultra-high-field fMRI in clinical applications.

In respect to more direct clinical application, first experiments with a speech paradigm could

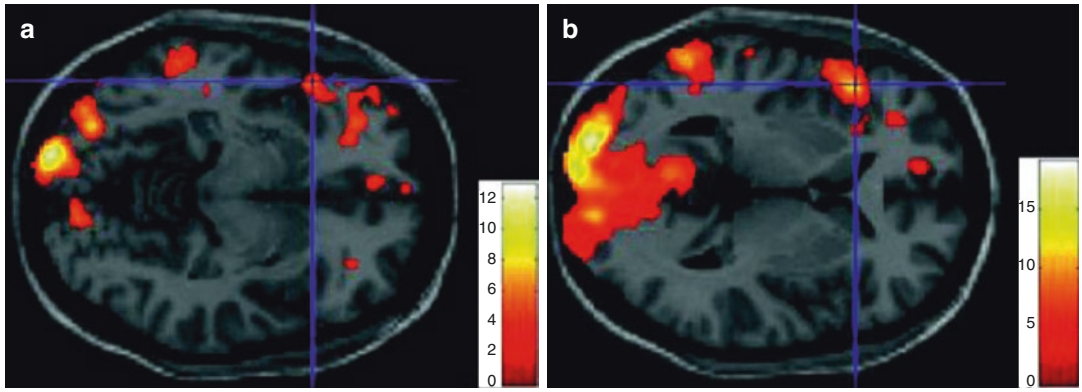

Fig. 4.7 Statistical parametric maps of activation within all subjects performing the verb-generation task compared with rest period at 1.5 T (**a**) and 7 T (**b**) superimposed on a standard brain in transverse orientation. Statistically corrected threshold is $p < 0.005$. Activated areas of Broca and Wernicke regions are shown at both field strengths but with more extended clusters and higher signal change at 7 T

reveal the advantages of 7-T fMRI combined with an 8-channel head coil and a parallel acquisition technique (Fig. 4.7). Even using the parallel acquisition technique, an increase in BOLD signal could be obtained, and a more extended activation and detection of lateralization could be found. Furthermore, the application of parallel imaging led to a significant reduction of artefacts (Fig. 4.2). Therefore, a reliable co-registration of high-resolution structural images with the EPI images could be performed. Figure 4.8 shows a patient with a cavernoma scanned pre-surgically at 1.5 T (a) and 7 T (b). The speech paradigm was a verb-generation task in both measurements in a block design. The activation maps are superimposed on susceptibility-weighted images (SWI) at 1.5 and 7 T. In addition to the higher BOLD signal and the more extended activation at 7 T, the higher spatial resolution of the structural images confers further benefit for surgical planning. One recent study could demonstrate the clinical benefit of 7-T fMRI. The primary motor hand area was analysed at 3 and 7 T in 17 patients (Beisteiner and Robinson 2011). However, as in former studies, 7-T data suffered from significant increase of artefacts (ghosting, head motion).

With the higher resolution and further optimized sequences, spinal cord structures come to the focus of interest. Recently, a group reported their findings of resting-state functional connectivity in the human spinal cord in a cohort of healthy volunteers. They observed robust functional connectivity between left and right ventral motor horns and between left and right dorsal sensory horns (Barry et al. 2016).

Besides fundamental experimental interests, e.g. for cognitive studies, clinical indications of 7-T fMRI can be imagined. Pre-surgical fMRI in patients with brain tumours could benefit from either higher resolution or faster imaging. Even patients impaired with respect to motor function are for the most part able to perform a short-finger movement sufficient for a single-block examination.

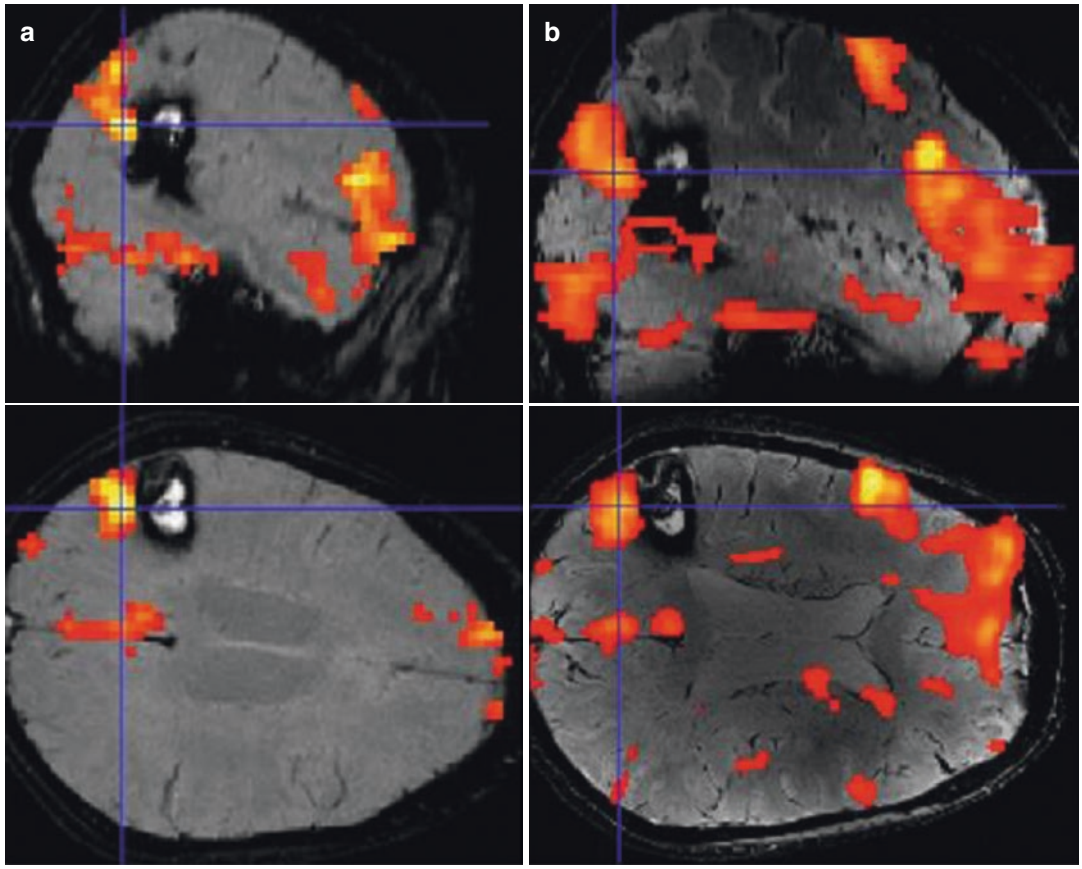

Fig. 4.8 Statistical parametric maps of activation within one patient performing the verb-generation task compared with rest period at 1.5 T (**a**) and 7 T (**b**) superimposed on SWI images. Statistically corrected threshold is $p < 0.005$. Activated areas of Broca and Wernicke regions are shown at both field strengths but with more extended clusters and higher signal change at 7 T. Furthermore, the structural images have a higher in-plane resolution at 7 T with enhanced tumour-brain differentiation and superior depiction of the inner structure of the cavernoma

References

Alvarez-Linera J (2008) 3 T MRI: advances in brain imaging. Eur J Radiol 67(3):415–426

Andersson P, Ramsey NF et al (2010) BCI control using 4 direction spatial visual attention and real-time fMRI at 7 T. Conf Proc IEEE Eng Med Biol Soc 2010:4221–4225

Banks SJ, Jones-Gotman M et al (2012) Sex differences in the medial temporal lobe during encoding and recognition of pseudowords and abstract designs. NeuroImage 59(2):1888–1895

Barry RL, Strother SC (2011) Data-driven optimization and evaluation of 2D EPI and 3D PRESTO for BOLD fMRI at 7 Tesla: I. Focal coverage. NeuroImage 55(3):1034–1043

Barry RL, Rogers BP, Conrad BN, Smith SA, Gore JC (2016) Reproducibility of resting state spinal cord networks in healthy volunteers at 7 Tesla. NeuroImage 133:31–40

Bednařík P, Tkáč I, Giove F, DiNuzzo M, Deelchand DK, Emir UE, Eberly LE, Mangia S (2015 Mar 31) Neurochemical and BOLD responses during neuronal activation measured in the human visual cortex at 7 Tesla. J Cereb Blood Flow Metab 35(4):601–610

Beisteiner R, Robinson S (2011) Clinical fMRI: evidence for a 7T benefit over 3T. NeuroImage 57(3):1015–1021

Bianciardi M, Toschi N, Eichner C, Polimeni JR, Setsompop K, Brown EN, Hämäläinen MS, Rosen BR, Wald LL (2016 Jun) In vivo functional connectome of human brainstem nuclei of the ascending arousal, autonomic, and motor systems by high spatial resolution 7-Tesla fMRI. MAGMA 29(3):451–462

Blatow M, Reinhardt J et al (2011) Clinical functional MRI of sensorimotor cortex using passive motor and sensory stimulation at 3 Tesla. J Magn Reson Imaging 34(2):429–437

Brunheim S, Johst S, Pfaffenrot V, Maderwald S, Quick HH, Poser BA (2017 Dec) Variable slice thickness (VAST) EPI for the reduction of susceptibility artifacts in whole-brain GE-EPI at 7 Tesla. MAGMA 30(6):591–607

Chang P, Nassirpour S, Henning A (2018 Jan) Modeling real shim fields for very high degree (and order) B0 shimming of the human brain at 9.4 T. Magn Reson Med 79(1):529–540

de Hollander G, Keuken MC, van der Zwaag W, Forstmann BU, Trampel R (2017 Jun) Comparing functional MRI protocols for small, iron-rich basal ganglia nuclei such as the subthalamic nucleus at 7 T and 3 T. Hum Brain Mapp 38(6):3226–3248

De Martino F, Esposito F (2011) Whole brain high-resolution functional imaging at ultra high magnetic fields: an application to the analysis of resting state networks. NeuroImage 57(3):1031–1044

Deistung A, Schäfer A, Schweser F, Biedermann U, Güllmar D, Trampel R, Turner R, Reichenbach JR (2013) High-resolution MR imaging of the human brainstem in vivo at 7 Tesla. Front Hum Neurosci 7:710

Duong TQ, Yacoub E et al (2003) Microvascular BOLD contribution at 4 and 7 T in the human brain: gradient-echo and spin-echo fMRI with suppression of blood effects. Magn Reson Med 49(6):1019–1027

Faull OK, Jenkinson M, Clare S, Pattinson KT (2015 Jun) Functional subdivision of the human periaqueductal grey in respiratory control using 7 Tesla fMRI. NeuroImage 113:356–364

Gizewski ER, de Greiff A et al (2007) FMRI at 7 T: whole-brain coverage and signal advantages even infratentorially? NeuroImage 37(3):761–768

Gizewski ER, Maderwald S, Linn J, Dassinger B, Bochmann K, Forsting M, Ladd ME (2014 Mar) High-resolution anatomy of the human brain stem using 7-T MRI: improved detection of inner structures and nerves? Neuroradiology 56(3):177–186

Goodyear BG, Douglas EA (2008) Minimum detectable change in motor and prefrontal cortex activity over repeated sessions using 3 T functional MRI and a block design. J Magn Reson Imaging 28(5):1055–1060

Gowland PA, Bowtell R (2007) Theoretical optimization of multi-echo fMRI data acquisition. Phys Med Biol 52(7):1801–1813

Hale JR, Brookes MJ (2010) Comparison of functional connectivity in default mode and sensorimotor networks at 3 and 7 T. MAGMA 23(5–6):339–349

Heid O (1997) Robust EPI phase correction. In: Proceedings of the ISMRM, Vancouver, 1997

Hoffmann MB, Stadler J et al (2009) Retinotopic mapping of the human visual cortex at a magnetic field strength of 7 T. Clin Neurophysiol 120(1):108–116

Hua J, Qin Q, van Zijl PC, Pekar JJ, Jones CK (2014 Dec) Whole-brain three-dimensional T2-weighted BOLD functional magnetic resonance imaging at 7 Tesla. Magn Reson Med 72(6):1530–1540

Jeon HA, Anwander A, Friederici AD (2014 Jul 9) Functional network mirrored in the prefrontal cortex, caudate nucleus, and thalamus: high-resolution functional imaging and structural connectivity. J Neurosci 34(28):9202–9212

Juchem C, Nixon TW, McIntyre S, Boer VO, Rothman DL, de Graaf RA (2011 Oct) Dynamic multi-coil shimming of the human brain at 7 T. J Magn Reson 212(2):280–288

Juchem C, Umesh Rudrapatna S, Nixon TW, de Graaf RA (2015 Jan 15) Dynamic multi-coil technique (DYNAMITE) shimming for echo-planar imaging of the human brain at 7 Tesla. NeuroImage 105:462–472

Kemper VG, De Martino F, Yacoub E, Goebel R (2016 Sep) Variable flip angle 3D-GRASE for high resolution fMRI at 7 Tesla. Magn Reson Med 76(3):897–904

Kim T, Lee Y, Zhao T, Hetherington HP, Pan JW (2017 Nov) Gradient-echo EPI using a high-degree shim insert coil at 7 T: implications for BOLD fMRI. Magn Reson Med 78(5):1734–1745

Kohn N, Kellermann T et al (2011) Gender differences in the neural correlates of humor processing: implications for different processing modes. Neuropsychologia 49(5):888–897

Ladd ME (2007) High-field-strength magnetic resonance: potential and limits. Top Magn Reson Imaging 18(2):139–152

Lee S, Polimeni JR, Price CM, Edlow BL, McNab JA (2018 Jun) Characterizing signals within lesions and mapping brain network connectivity after traumatic axonal injury: a 7 Tesla resting-state FMRI study. Brain Connect 8(5):288–298

Lenglet C, Abosch A, Yacoub E, De Martino F, Sapiro G, Harel N (2012) Comprehensive in vivo mapping of the human basal ganglia and thalamic connectome in individuals using 7T MRI. PLoS One 7(1):e29153

Lewis LD, Setsompop K, Rosen BR, Polimeni JR (2018 Jun 20) Stimulus-dependent hemodynamic response timing across the human subcortical-cortical visual pathway identified through high spatiotemporal resolution 7T fMRI. NeuroImage 181:279–291

Malekian V, Nasiraei-Moghaddam A, Khajehim M (2018 Jul) A robust SSFP technique for fMRI at ultra-high field strengths. Magn Reson Imaging 50:17–25

Martuzzi R, van der Zwaag W, Farthouat J, Gruetter R, Blanke O (2014 Jan) Human finger somatotopy in areas 3b, 1, and 2: a 7T fMRI study using a natural stimulus. Hum Brain Mapp 35(1):213–226

Mirrashed F, Sharp JC et al (2004) High-resolution imaging at 3 T and 7 T with multiring local volume coils. MAGMA 16(4):167–173

Newton AT, Rogers BP et al (2012) Improving measurement of functional connectivity through decreasing partial volume effects at 7 T. NeuroImage 59(3):2511–2517

Norris DG (2003) High field human imaging. J Magn Reson Imaging 18(5):519–529

Okada T, Yamada H et al (2005) Magnetic field strength increase yields significantly greater contrast-to-noise ratio increase: measured using BOLD contrast in the primary visual area. Acad Radiol 12(2):142–147

Olman CA, Van de Moortele PF et al (2010) Retinotopic mapping with spin echo BOLD at 7 T. Magn Reson Imaging 28(9):1258–1269

Olman CA, Pickett KA et al (2012) Selective BOLD responses to individual finger movement measured with fMRI at 3 T. Hum Brain Mapp 33(7): 1594–1606

Pfeuffer J, Adriany G et al (2002a) Perfusion-based high-resolution functional imaging in the human brain at 7 Tesla. Magn Reson Med 47(5):903–911

Pfeuffer J, Van de Moortele PF et al (2002b) Correction of physiologically induced global off-resonance effects in dynamic echo-planar and spiral functional imaging. Magn Reson Med 47(2):344–353

Pfeuffer J, Van de Moortele PF et al (2002c) Zoomed functional imaging in the human brain at 7 Tesla with simultaneous high spatial and high temporal resolution. NeuroImage 17(1):272–282

Pohmann R, Speck O, Scheffler K (2016 Feb) Signal-to-noise ratio and MR tissue parameters in human brain imaging at 3, 7, and 9.4 Tesla using current receive coil arrays. Magn Reson Med 75(2):801–809

Polimeni JR, Fischl B et al (2010) Laminar analysis of 7 T BOLD using an imposed spatial activation pattern in human V1. NeuroImage 52(4):1334–1346

Poser BA, Versluis MJ et al (2006) BOLD contrast sensitivity enhancement and artifact reduction with multiecho EPI: parallel-acquired inhomogeneity-desensitized fMRI. Magn Reson Med 55(6):1227–1235

Preibisch C, Wallenhorst T et al (2008) Comparison of parallel acquisition techniques generalized autocalibrating partially parallel acquisitions (GRAPPA) and modified sensitivity encoding (mSENSE) in functional MRI (fMRI) at 3 T. J Magn Reson Imaging 27(3):590–598

Sanchez Panchuelo RM, Ackerley R, Glover PM, Bowtell RW, Wessberg J, Francis ST, McGlone F (2016) Mapping quantal touch using 7 Tesla functional magnetic resonance imaging and single-unit intraneural microstimulation. Elife 5. pii: e12812

Sanchez-Panchuelo RM, Schluppeck D (2010) Mapping human somatosensory cortex in individual subjects with 7T functional MRI. J Neurophysiol 103(5):2544–2556. https://doi.org/10.1152/jn.01017.2009

Scheef L, Landsberg MW et al (2007) Methodological aspects of functional neuroimaging at high field strength: a critical review. Rofo 179(9):925–931

Scheffler K, Ehses P (2016 Jul) High-resolution mapping of neuronal activation with balanced SSFP at 9.4 Tesla. Magn Reson Med 76(1):163–171

Schlamann M, Voigt MA et al (2010a) Exposure to high-field MRI does not affect cognitive function. J Magn Reson Imaging 31(5):1061–1066

Schlamann M, Yoon MS et al (2010b) Short term effects of magnetic resonance imaging on excitability of the motor cortex at 1.5 T and 7 T. Acad Radiol 17(3):277–281

Sengupta S, Roebroeck A, Kemper VG, Poser BA, Zimmermann J, Goebel R, Adriany G (2016) A specialized multi-transmit head coil for high resolution fMRI of the human visual cortex at 7T. PLoS One.11(12):e0165418

Shah P, Bassett DS, Wisse LEM, Detre JA, Stein JM, Yushkevich PA, Shinohara RT, Pluta JB, Valenciano E, Daffner M, Wolk DA, Elliott MA, Litt B, Davis KA, Das SR (2018 Feb) Mapping the structural and functional network architecture of the medial temporal lobe using 7T MRI. Hum Brain Mapp 39(2):851–865

Shimada Y, Kochiyama T et al (2008) System stability of a 3 T-MRI during continuous EPI scan. Nippon Hoshasen Gijutsu Gakkai Zasshi 64(12):1504–1512

Theysohn JM, Maderwald S et al (2008) Subjective acceptance of 7 Tesla MRI for human imaging. MAGMA 21(1–2):63–72

Theysohn N, Qin S, Maderwald S, Poser BA, Theysohn JM, Ladd ME, Norris DG, Gizewski ER, Fernandez G, Tendolkar I (2013 Oct) Memory-related hippocampal activity can be measured robustly using FMRI at 7 Tesla. J Neuroimaging 23(4):445–451

Thürling M, Küper M et al (2011) Activation of the dentate nucleus in a verb generation task: a 7 T MRI study. NeuroImage 57(3):1184–1191

Torrisi S, O'Connell K, Davis A, Reynolds R, Balderston N, Fudge JL, Grillon C, Ernst M (2015 Oct) Resting state connectivity of the bed nucleus of the stria terminalis at ultra-high field. Hum Brain Mapp 36(10):4076–4088

Triantafyllou C, Hoge RD et al (2005) Comparison of physiological noise at 1.5 T, 3 T and 7 T and optimization of fMRI acquisition parameters. NeuroImage 26(1):243–250

Triantafyllou C, Hoge RD et al (2006) Effect of spatial smoothing on physiological noise in high-resolution fMRI. NeuroImage 32(2):551–557

van der Zwaag W, Marques JP et al (2009) Minimization of Nyquist ghosting for echo-planar imaging at ultra-high fields based on a "negative readout gradient" strategy. J Magn Reson Imaging 30(5):1171–1178

van der Zwaag W, Marques JP et al (2012) Temporal SNR characteristics in segmented 3D-EPI at 7 T. Magn Reson Med 67(2):344–352

Vaughan JT, Garwood M et al (2001) 7 T vs. 4 T: RF power, homogeneity, and signal-to-noise comparison in head images. Magn Reson Med 46(1):24–30

Walter M, Stadler J et al (2008) High resolution fMRI of subcortical regions during visual erotic stimulation at 7 T. MAGMA 21(1–2):103–111

Wiggins GC, Potthast A et al (2005) Eight-channel phased array coil and detunable TEM volume coil for 7 T brain imaging. Magn Reson Med 54(1): 235–240

Yacoub E, Hu X (2001) Detection of the early decrease in fMRI signal in the motor area. Magn Reson Med 45(2):184–190

Yacoub E, Shmuel A et al (2001) Imaging brain function in humans at 7 Tesla. Magn Reson Med 45(4): 588–594

Yacoub E, Duong TQ et al (2003) Spin-echo fMRI in humans using high spatial resolutions and high magnetic fields. Magn Reson Med 49(4):655–664

Zou KH, Greve DN et al (2005) Reproducibility of functional MR imaging: preliminary results of prospective multi-institutional study performed by biomedical informatics research network. Radiology 237(3):781–789